Flexoelectric enhancement in lead-free piezocomposites with graded inclusion concentrations and porous matrices

Jagdish A. Krishnaswamy, Federico C. Buroni, Roderick Melnik, Luis Rodriguez-Tembleque, and Andres Saez

Computers and Structures, 289, 107176, 2023.
DOI: 10.1016/j.compstruc.2023.107176

Highlights

- The key factors influencing flexoelectric enhancement in piezocomposites have been explored, with the main focus given to lead-free piezoelectric composite materials.

- Using an advanced electro-elastic model that incorporates piezoelectric and flexoelectric couplings, two novel design proposals that allow flexoelectric enhancement in lead-free piezocomposites have been investigated in detail.

- Computational analysis has included important cases of introducing anisotropy into the composite structure through a graded inclusion concentration, as well as introducing porosity in the matrix to create structural anisotropy.

- The developed strategies have demonstrated their capability of generating significant size-dependent flexoelectric enhancements.

- This work paves a way for newer manufacturing-compatible techniques to optimize the performance of the functional electro-elastic composite materials that are crucial for lead-free and environmentally friendly technologies.

Abstract

Flexoelectricity is the generation of electric fields through strain gradients. It offers unconventional ways to enhance the electromechanical coupling response of piezoelectric materials and composites compared to the conventional piezoelectricity which is a coupling between strain and electric fields. While the factors that are crucial for designing and tailoring flexoelectric enhancement have been explored from a perspective of bulk-piezoelectric materials, the factors influencing flexoelectric enhancement in piezo-composites are scarcely explored. Here, we investigate two design proposals to introduce flexoelectric enhancement in lead-free piezocomposites using an advanced electro-elastic model that incorporates piezoelectric and flexoelectric couplings. The first idea involves introducing anisotropy into the composite structure through a graded inclusion concentration. The second idea involves introducing porosity in the matrix to create structural anisotropy. We show that both of these strategies are capable of generating significant size-dependent flexoelectric enhancements. In summary, this investigation paves a way for newer manufacturing-compatible techniques to optimize the performance of the functional electro-elastic composite materials that are crucial for lead-free and environmentally friendly technologies.

==

Keywords

Lead-free piezocomposites; flexoelectricity; nonlocal size-dependent effects; green economy and eco-friendly technologies; coupled models; composite structures

Flexoelectric enhancement in lead-free piezocomposites with graded inclusion concentrations and porous matrices

Jagdish A. Krishnaswamy[1], Federico C. Buroni[2], Roderick Melnik[1,3], Luis Rodriguez-Tembleque[3], Andres Saez[3]

[1]MS2Discovery Interdisciplinary Research Institute, Wilfrid Laurier University, 75 University Ave W, Waterloo, Ontario, Canada, N2L 3C5

[2]Department of Mechanical Engineering and Manufacturing, Universidad de Sevilla, Camino de los Descubrimientos s/n, Seville E-41092, Spain

[3]Department of Continuum Mechanics and Structural Analysis, Universidad de Sevilla, Camino de los Descubrimientos s/n, Seville E-41092, Spain

Abstract

Flexoelectricity is the generation of electric fields through strain gradients. It offers unconventional ways to enhance the electromechanical coupling response of piezoelectric materials and composites compared to the conventional piezoelectricity which is a coupling between strain and electric fields. While the factors that are crucial for designing and tailoring flexoelectric enhancement have been explored from a perspective of bulk-piezoelectric materials, the factors influencing flexoelectric enhancement in piezo-composites are scarcely explored. Here, we investigate two design proposals to introduce flexoelectric enhancement in lead-free piezocomposites using an advanced electro-elastic model that incorporates piezoelectric and flexoelectric couplings. The first idea involves introducing anisotropy into the composite structure through a graded inclusion concentration. The second idea involves introducing porosity in the matrix to create structural anisotropy. We show that both of these strategies are capable of generating significant size-dependent flexoelectric enhancements. In summary, this investigation paves a way for newer manufacturing-compatible techniques to optimize the performance of the functional electro-elastic composite materials that are crucial for lead-free and environmentally friendly technologies.

Keywords: Lead-free piezocomposites, flexoelectricity, electro-elastic coupling, nonlocal size-dependent effects, coupled models, finite element analysis, composite structures.

1. Introduction

Lead-free piezoelectric composite materials have attracted attention as potential replacements to lead-based materials that are currently used widely to manufacture electromechanical sensors and actuators, energy harvesting, as well as in many other engineering applications [1], [2]. However, it is important to highlight that the performance deficits that are brought about by these materials need to be compensated through newer, often unconventional, ways of material and structural design. Some of the ways in which this challenge has been addressed in research involves tuning the crystallinity (or polycrystallinity) of the piezoelectric material [3]–[6], introducing nano-additives into the matrix to enhance both the elastic and the dielectric properties of the matrix and the composite [5]–[7], introduction of auxetic structures to enhance the piezoelectric coupling [8], [9] and so on. Besides these approaches, we have certain pathways that are often overlooked but could yield considerable scope for enhanced electromechanical coupling. One of these approaches is to enhance the flexoelectric coupling. Flexoelectricity involves the generation of electricity from strain gradients as opposed to the strain and electric field coupling in piezoelectricity. However, introducing strain gradients in a composite is not straightforward. For example, a composite structure in which piezoelectric inclusions are homogeneously dispersed cannot offer significant flexoelectric enhancement. This is because the structure lacks the structural anisotropy that is fundamental to the creation of strain gradients on application of an external mechanical stimulus. Flexoelectricity is a nonlocal effect that has been investigated in the context of bulk piezoelectric materials [10]–[13] . Anisotropic structures such as truncated pyramids (in three dimensions) and truncated triangles (in two dimensions) have been shown to introduce the required anisotropy that brings about strain gradients. We earlier demonstrated that this approach can be extended to lead-free piezoelectric composites also [14]. Some of the major applications of piezocomposites are in the form of sensors, actuators, and energy harvesters in the contexts of wearable and stretchable devices for human integration and soft robotics. These applications require soft, stretchable, and compliant devices [15]. Therefore, conventional methods of hardening the piezocomposite matrix might not lead to a suitable strategy to boost the piezoelectric response. Further, considering the large-area nature of these devices, it is crucial to investigate material structures that are amenable to easy fabrication and manufacturing. Towards addressing this challenge, we will be revisiting flexoelectric design principles that can help improving the effective piezoelectric response without hardening the composite material. The approaches developed here can also be adapted for scalable fabrication because the structural and compositional modifications introduced in the composite can be implemented through tuning of fabrication parameters considering emerging manufacturing techniques such as three-dimensional printing.

In this direction, here, we investigate two design proposals to introduce flexoelectric coupling in lead-free piezocomposites. Both of these approaches are based on tuning the internal structure of a composite whose external boundary is regular otherwise, e.g. rectangular (in two dimensions). This is consonant with the idea to use conventional methods to design regular manufacturable shapes such as piezoelectric composite slabs, films, and so on which have no irregular outer boundaries that might pose fabrication difficulties. However, by tuning the manufacturing parameters during the process of fabricating the composite material, the details of the internal structure can be controlled. This can be used to bring about controlled anisotropy in the internal structure of the composite at the time of manufacturing. Hence, the proposals we investigate here consider two possibilities along these lines – controlling the piezoelectric inclusion concentration distribution and controlling the porosity of the matrix material. As we shall see, both these approaches allow well-pronounced flexoelectric enhancements at small-size scales. The rest of the paper is organized as follows. In section 2, we introduce the electro-elastic model that combines the linear piezoelectric, flexoelectric, and nonlinear electrostrictive couplings along with the boundary conditions and material properties relevant to our study. In section 3, we apply this coupled model to investigate the two design proposals discussed above and, subsequently, we discuss the essential design rules that emerge out of these designs. In section 4, we provide a summary of the findings with comments for future work.

2. Electro-elastic model, effective electro-elastic coefficients, and boundary conditions

Our starting point is based on the theoretical coupled models that describe the different forms of electromechanical coupling in piezoelectric composites. The approach taken here is to develop a model that describes, along with linear piezoelectric coupling, additional important modes of coupling that include non-linear electrostriction and size-dependent piezoelectricity. The latter has also been motivated by the works on hierarchical small-scale material architectures that provide multiple possibilities for enhanced piezoelectric performance in lead-free piezoelectrics [16], [17], making flexoelectricity a natural candidate to explore for such enhancements at small scales. We will further look at the generic representative volume element (RVE) and the boundary conditions that are applied to it to simulate and obtain the effective piezoelectric parameters as a function of a size-scale parameter.

2.1. Coupled electro-elastic model

In what follows, we will develop an electro-elastic coupled model that includes the next modes of coupling: flexoelectricity (coupling between strain-gradient and electric fields), electrostriction (second order nonlinear coupling between strain and electric field), and linear piezoelectricity (coupling between strain and electric field). We will start with a generic Gibbs free energy function that has contributions due to all these phenomena which is expressed as [18]–[21]:

$$G = \frac{1}{2} c_{ijkl}\varepsilon_{ij}\varepsilon_{kl} - \frac{1}{2}\epsilon_{ij}E_iE_j - e_{kij}E_k\varepsilon_{ij} - \frac{1}{2}B_{klij}E_kE_l\varepsilon_{ij} - \mu_{ijkl}E_i\varepsilon_{jk,l}. \quad (1)$$

where, c_{ijkl}, ϵ_{ij}, e_{ijk}, B_{ijkl}, and μ_{ijkl} are the material parameters including, in order, the elastic coefficients, the permittivity, the piezoelectric, electrostrictive, and flexoelectric coefficients. Further, ε_{ij}, E_i, and $\varepsilon_{jk,l}$ are the components of the strain tensor, electric field, and the strain-gradient. Linear piezoelectric models which are traditionally considered for modelling piezocomposite behaviour would not incorporate the components due to the electrostriction $\left(-\frac{1}{2}B_{klij}E_kE_l\varepsilon_{ij}\right)$ and flexoelectricity $\left(-\mu_{ijkl}E_i\varepsilon_{jk,l}\right)$ and the free energy function in such cases would be $G = \frac{1}{2}c_{ijkl}\varepsilon_{ij}\varepsilon_{kl} - \frac{1}{2}\epsilon_{ij}E_iE_j - e_{kij}E_k\varepsilon_{ij}$ [22].

Usually, the free energy function would also include a term involving the product of pairs of strain gradient components to model size-dependent elasticity [23], [24][25], [26]. However, we note that these effects operate at a size-scale of 1-10 nm [27]. Given that we consider length scales which are at least an order of magnitude larger than these scales, we neglect this coupled effect in our model.

Using the free energy function given in Eq. (1), we derive the phenomenological relations describing the electro-elastic behaviour of piezocomposites as:

$$\sigma_{ij} = \frac{\partial G}{\partial \varepsilon_{ij}} = c_{ijkl}\varepsilon_{kl} - e_{kij}E_k - \frac{1}{2}B_{klij}E_kE_l, \quad (2)$$

$$\hat{\sigma}_{ijk} = \frac{\partial G}{\partial \varepsilon_{ij,k}} = -\mu_{lijk}E_l, \quad (3)$$

$$D_i = -\frac{\partial G}{\partial E_i} = \epsilon_{ij}E_j + e_{ijk}\varepsilon_{jk} + B_{ijkl}E_j\varepsilon_{kl} + \mu_{ijkl}\varepsilon_{jk,l}. \quad (4)$$

In the above equations, σ_{ij}, $\hat{\sigma}_{ijk}$ and D_i are components of the standard stress tensor, the higher order stress tensor, and electric flux density, respectively. Furthermore, the above phenomenological relations are subjected to the following governing balance equations given by [10], [11]:

$$\left(\sigma_{ij} - \widehat{\sigma}_{ijk,k}\right)_{,j} + F_i = 0, \tag{5}$$

$$D_{i,i} = 0, \tag{6}$$

where F_i are the body force components, which are assumed to vanish in our model. The phenomenological relations are substituted in the governing equations and the resulting system of nonlinear, nonlocal differential equations are solved using the finite element method. The strain and displacement components are, further, linked to each other by the Cauchy relationship $\varepsilon_{ij} = \frac{1}{2}(u_{i,j} + u_{j,i})$ and the electric field is the negative gradient of the electric potential (i.e. $E_i = -V_{,i}$).

2.2. RVE geometry

We consider a two-dimensional RVE with sides a_m and b_m as shown in Figure 1(a), as a representative example. The actual internal structural and compositional details will change depending on the scenario under study. For example, in our studies, we would consider a graded inclusion concentration in one case and a porous matrix in another. The boundary conditions and the overall unit cell dimensions will remain the same in all these cases. Therefore, this figure serves as a common illustration of these factors that describe the conditions pertaining to the unit cell dimensions and its boundaries that are common in all the examples. Inclusions have random shapes that are constrained within concentric circles with radii R_1 and R_2 ($R_2 > R_1$). To simulate size dependent electroelastic coupling behaviour, we scale the length scales along both the x and y axes by a factor N, such that the scaled RVE would have sides Na_m and Nb_m. The reference RVE with $N = 1$ has dimensions $a_m = b_m = 50\mu\text{m}$ with R_1 and R_2 picked randomly within the ranges [2.5-3.5 μm] and [4.0-5.0 μm], respectively. Applying the scaling factor on the composite architecture scales both the matrix dimensions (a_m and b_m) and the inclusion radii (R_1 and R_2) by the same factor.

2.3. Boundary conditions

Figure 1(b) and (c) illustrate the boundary conditions used to compute the effective piezoelectric coefficients e_{31} and e_{33}, respectively, of the lead-free piezocomposite analyzed here in detail [28], [29] . Specifically, this approach shows agreement [29] with well-established flexoelectric characteristics of standard tapered geometries [19] . Lagrange quadratic shape functions are used for the dependent variables u_1, u_2 and V because it is seen that second order functions typically used in flexoelectric simulations for better representing the physical model [30] . We also note that C1-continuity can be obtained by other methodologies, such as using NURBS basis functions. These methodologies have already been discussed in the literature, along with the use of different types of boundary conditions, where the interested reader can find further details (e.g. [31]–[34])

Here, the boundary strains $\overline{\varepsilon_{11}}$ and $\overline{\varepsilon_{33}}$ which are set to a small value of 1×10^{-6}. For a parameter A, its volume average $\langle A \rangle$ over the RVE is given by:

$$\langle A \rangle = \frac{1}{a_m b_m} \int_\Omega A d\Omega. \tag{7}$$

The boundary conditions shown in Figure 1(a) yield the following volume averages:

$$\langle \varepsilon_{11} \rangle = \overline{\varepsilon_{11}}\,, \; \langle \varepsilon_{33} \rangle = 0, \langle \varepsilon_{13} \rangle = 0, \langle E_i \rangle = 0. \tag{8}$$

Similarly, the boundary condition in Figure 1(b) gives:

$$\langle \varepsilon_{11} \rangle = 0\,, \langle \varepsilon_{33} \rangle = \overline{\varepsilon_{33}}, \langle \varepsilon_{13} \rangle = 0\,, \langle E_i \rangle = 0. \tag{9}$$

After carrying out finite element simulations with these boundary conditions, the effective piezoelectric coefficients are calculated as [35]:

$$e_{31} = \frac{\langle D_3 \rangle}{\overline{\varepsilon_{11}}} \;,\; e_{33} = \frac{\langle D_3 \rangle}{\overline{\varepsilon_{33}}}. \tag{10}$$

where $\langle D_3 \rangle$ is the volume average of the D_3 component of the electric flux density vector.

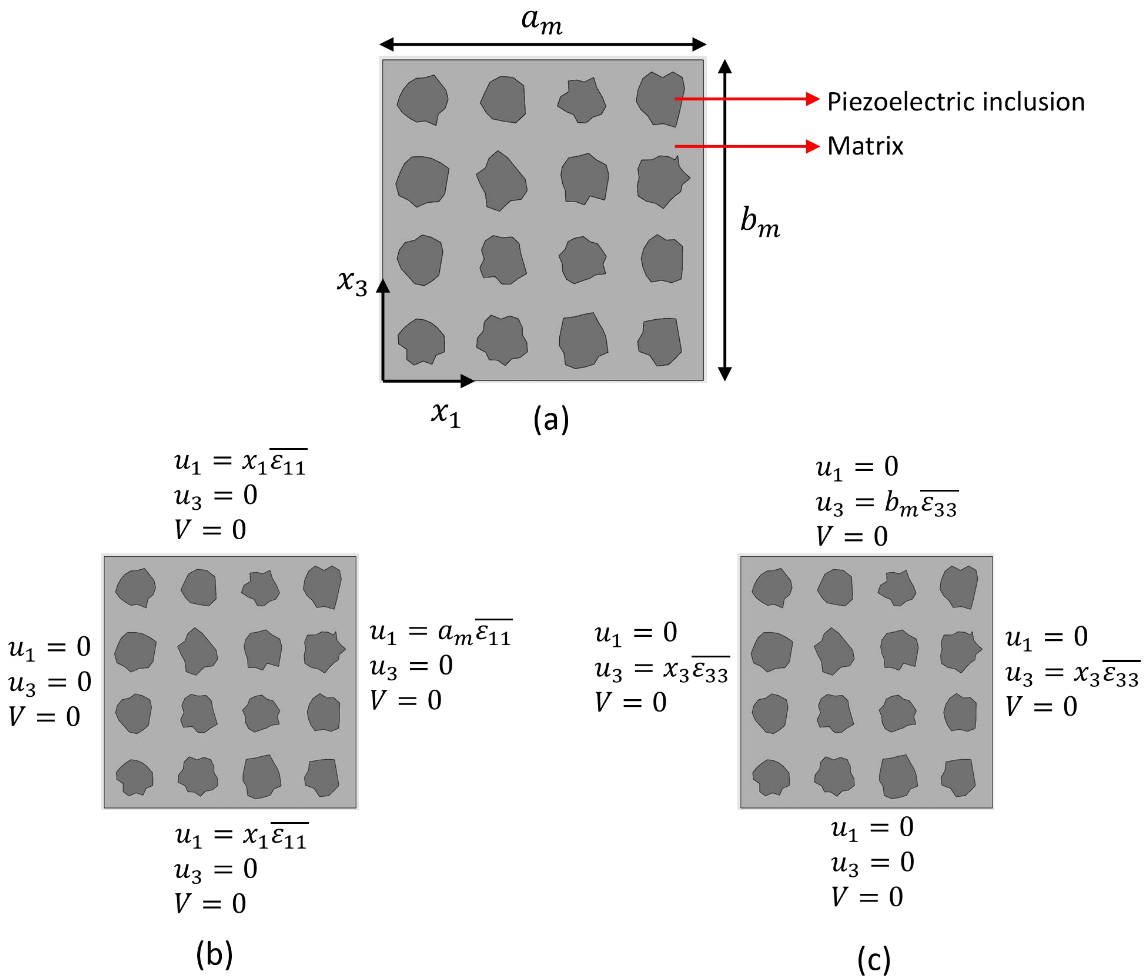

Figure 1 – (a) Representative illustration of a unit cell of a lead-free piezocomposite having a matrix in which piezoelectric inclusions are dispersed, (b) and (c) illustrate the boundary conditions that the displacement components u_1 and u_3, and the electric potential V are subjected to, to compute the effective piezoelectric coefficients e_{31} and e_{33}, respectively. $\overline{\varepsilon_{11}}$ and $\overline{\varepsilon_{33}}$ are boundary strains which are set to small values of 1×10^{-6}.

2.4. Material properties

Table 1, further, shows the material properties adopted for the study. We choose microscale piezoelectric $BaTiO_3$ inclusions which would allow grain sizes congenial to maximal piezoelectric coupling. This is an important design consideration for efficient devices such as strain sensors, electromechanical actuators, and so on. Some other applications, e.g. those encountered in haptic technologies, may favour piezoelectric inclusions from BNT or KNN lead-free material groups due to temperature considerations [17], [36] . Our results on the model development reported here can be generalized to such cases as well. Polycrystalline $BaTiO_3$ inclusions have piezoelectric coefficients that are functions of domain orientation which, to a first approximation, can be coalesced into an orientation distribution parameter α, such that $\alpha \to 0$ corresponding to a monocrystalline perfectly oriented limit and $\alpha \to \infty$ corresponds to a random disoriented limit. While bulk $BaTiO_3$ polycrystals exhibit better piezoelectric response compared to a monocrystal, it is important to recall that in the consideration of $BaTiO_3$ inclusions in a polymer matrix, monocrystalline/perfectly oriented $BaTiO_3$ inclusions exhibit maximal piezo-response, assuming there are no other functional additives in the matrix [5]. Therefore, given that we are considering additive-free designs to preclude any compromises on the softness of the matrix, the main focus of our analysis is on perfectly oriented $BaTiO_3$ crystals with $\alpha = 0$. Further, the flexoelectric behaviour of polycrystalline materials is a topic of current interest and, consequently, we lack well-characterized data on the effects of polycrystallinity on flexoelectricity. Although polycrystals with smaller grain sizes have shown larger flexoelectric coefficients compared to single crystals [37] and defective and semiconducting $BaTiO_3$ have been shown to exhibit a stronger sensitive to strain gradients [38], given our limited understanding of the influence of the polycrystalline nature of the inclusions on the flexoelectricity, we restrict our study to single crystals of $BaTiO_3$ that do no have polar gradient boundaries or vacancy defects.

Further, for our study, we consider a generic matrix material which has elastic moduli, E_m, ranging across three orders of magnitude starting from soft hydrogel-like matrices ($\sim 10^6$Pa) [39] up to epoxy-like matrices ($\sim 10^9$Pa) [40]. Moreover, we consider compressible matrices with a regular Poisson's ratio of $\nu_m = 0.35$ and incompressible matrices, such as PDMS (polydimethylsiloxane), having a Poisson's ratio of $\nu_m = 0.499$ [41]. The incompressibility of PDMS is a valid assumption when the strains are small [42], which corresponds to the nature of our analysis because we restrict our studies currently to small strains. The idea behind this is that the first part of the study pertains to understanding the matrix properties that lead to maximal flexoelectric enhancements.

A simplified notation is used for the flexoelectric coefficients. Since these coefficients are specified for the cubic phase of $BaTiO_3$ [43], [44], there are only three independent coefficients – the longitudinal component ($\mu_{1111} = \mu_{2222} = \mu_{3333}$) denoted by μ_L, the transverse component ($\mu_{1221} = \mu_{1331} = \mu_{2112} = \mu_{3113} = \mu_{2332} = \mu_{3223}$) denoted by μ_T, and the shear component ($\mu_{1133} = \mu_{1122} = \mu_{2233} = \mu_{2121} = \mu_{3232} = \mu_{3131}$) denoted by μ_S. Further, the flexoelectric tensor satisfies the symmetry $\mu_{ijkl} = \mu_{ikjl}$ [44]. The polarization contributions arising due to the longitudinal, transverse, and shear components of flexoelectricity are given by:

$$P_1 = \mu_L \frac{\partial \varepsilon_{11}}{\partial x_1} + 2\mu_S \frac{\partial \varepsilon_{13}}{\partial x_3} + \mu_T \frac{\partial \varepsilon_{33}}{\partial x_1}, \tag{11a}$$

$$P_3 = \mu_L \frac{\partial \varepsilon_{33}}{\partial x_3} + 2\mu_S \frac{\partial \varepsilon_{13}}{\partial x_1} + \mu_T \frac{\partial \varepsilon_{11}}{\partial x_3}. \tag{11b}$$

As far as the flexoelectric coefficients of $BaTiO_3$ are concerned, we consider only the transverse and longitudinal coefficients, μ_T and μ_L, respectively, because they are experimentally well characterized [45]. The shear component μ_S is not well characterized [43] and hence we do not consider its effects in the model (i.e. $\mu_S = 0$). This assumption is further supported by the fact that although theoretical studies have tried to estimate the shear coefficients, there is significant disagreement in its value [46], [47]. This discrepancy will be a subject of a separate publication, whereas here the focus will be on the two novel guiding principles of piezocomposite design discussed in detail in the subsequent section.

The coefficients of electrostriction, B_{ijkl}, mentioned Eq. (1)-(4) are derived from the experimentally measured coefficients Q_{ijkl} or M_{ijkl} [48], [49]. These coefficients are two different ways of describing electrostrictive coupling in terms of the polarization vector components (P_i) and the electric field components (E_i), respectively. Specifically, these relations are given as [49]:

$$\varepsilon_{ij} = Q_{ijkl}P_kP_l, \tag{12a}$$

$$\varepsilon_{ij} = M_{ijkl}E_kE_l. \tag{12b}$$

It is possible to convert the above representation to another through the relation involving the dielectric susceptibility tensor components η_{ij}, as $M_{ijkl} = Q_{opkl}\eta_{oi}\eta_{pj}$[49]. Finally, to convert M_{ijkl} into B_{ijkl} to have compatibility with our free energy model (Eq. (1)), we need to apply the relation $B_{ijkl} = c_{ijpq}M_{pqkl}$ [50]. Computational difficulties related to stability are known to arise when studying non-linear and non-local effects simultaneously, specifically at smaller length scales. Hence, to be methodically clear, we focus here only the flexoelectric model in the absence of non-linear effects. However, it would be apt to point out that non-linear effects can be significant, specifically in architectures having larger inclusion concentrations and under larger strains.

Finally, the terms λ_m and μ_m in Table 1 describe the elastic behaviour of the isotropic matrix material such that $\lambda_m = \frac{E_m\nu_m}{(1+\nu_m)(1-2\nu_m)}$ and $\mu_m = \frac{E_m}{2(1+\nu_m)}$, where E_m and ν_m are the Young's modulus and Poisson's ratio, respectively, of the matrix material. The flexoelectric coefficients given in Table 1 are in the experimentally measured range.

Table 1 – Electro-elastic material properties used in the simulations and typical values of electrostrictive coefficients are considered for the polymer matrix

Material property	Values for $BaTiO_3$	Values for matrix
Elastic coefficients (Moduli in Pa)		
c_{11}	275.1×10^9 [51]	$\lambda_m + 2\mu_m$
c_{13}	151.55×10^9	λ_m
c_{33}	164.8×10^9	$\lambda_m + 2\mu_m$
c_{44}	54.3×10^9	μ_m
Young's modulus, E_m	N.A.	$[1 \times 10^6, 1 \times 10^9]$
Poisson's ratio, ν_m	N.A.	0.35 and 0.499
Relative permittivity		
ϵ_{11}/ϵ_0	1970 [51]	2.72 [24]
ϵ_{33}/ϵ_0	109	2.72
Piezoelectric coefficients (Cm^{-2})		
e_{15}	21.3 [51]	
e_{31}	-2.69	Matrix is non-piezoelectric
e_{33}	3.65	
Flexoelectric coefficients (Cm^{-1})		
Longitudinal, μ_L	1×10^{-6} [19], [43], [52]	1×10^{-9} [53]
Transverse, μ_T	1×10^{-6} [19], [43], [52]	1×10^{-9}
Shear, μ_S	-	-

3. Lead-free piezocomposite design experiments and results

We explore two piezocomposite designs considering the following guiding design principles:

1. **Retaining composite softness for wearable and soft-robotic applications:** This is important for many applications such as wearable electronics and soft-robotics. Having this in mind, in our analysis, we avoid introduction of nano-additives that harden the matrix and, further, we try to reduce or retain the piezoelectric inclusion concentration.
2. **Amenability to additive manufacturing:** We conceptualize composite architectures where the required structural and compositional variations can be introduced in a straightforward manner by tuning process parameters in a three-dimensional printer.

The proof-of-concept approach taken here brings in the structural and compositional designs required for flexoelectricity with an RVE that would be part of a larger design. However, one needs to keep in mind that in reality, the composite device would not have these RVEs as periodically repeating units. The variations would occur over larger device volumes. Therefore, the examples explored here are representative in their nature, with the intention of investigating the feasibility of flexoelectric enhancement and understanding the configurations that would help flexoelectric effect reinforce the existing linear piezoelectric effect. The latter is crucial to the development of efficient lead-free and ecologically-friendly technologies.

3.1. Size-dependent piezoelectric enhancements in piezocomposites with graded inclusion concentrations

In this section, we consider a design in which the spatial distribution of the $BaTiO_3$ inclusions in the matrix is non-uniform. In fact, we study an example where the inclusion concentration decreases along the x_3 direction (thickness direction) of the composite, as shown in Figure 2. This is one of many ways in which an inhomogeneous inclusion concentration can be introduced and we have chosen this setup as a proof-of-concept. The concentration gradient introduces an elastic gradient such that the effective elastic coefficients of the composite decreases along the x_3 direction, thus providing a way to introduce strain gradients under applied stresses which are otherwise uniform across different cross-sections of the composite. We undertake a procedure to boost the effective piezoelectricity by not filling up the matrix with piezoelectric inclusions homogeneously, but by spatially configuring a limited number of inclusions in a graded manner to introduce enhancements due to flexoelectricity. Therefore, the proposed design approach attempts to improve the piezoelectric response without the need to harden the matrix or to increase the inclusion concentration. Further, fabrication methods such as additive manufacturing can be tuned to introduce the structural and compositional anisotropy required to implement the design [54].

The average inclusion concentration in this case, within the RVE unit cell, is approximately $V_{BTO} = 23\%$. The inclusions are placed at random locations with the effective inclusion concentration reducing along the x_3 direction of the RVE. Our previous studies have shown that minor variations in the random positions of the inclusions do not affect the overall piezoelectric response in a statistically significant manner [5]. Based on this understanding, we consider the architecture in Figure 2 as a representative example of a functionally graded piezocomposite architecture which can potentially benefit from flexoelectric contributions. The matrix dimensions and the boundary conditions used to compute the effective piezoelectric parameters are as explained in section 2.

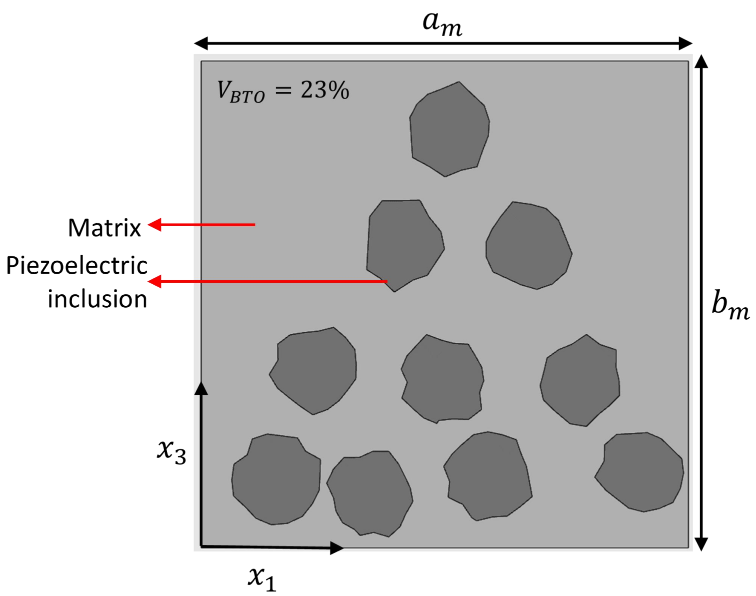

Figure 2 – RVE of an example unit cell of a piezocomposite with graded inclusion concentration considered in this section.

The size dependent piezoelectric properties of this material structure are computed by varying the size scale N, as explained in section 2, across a range of values that span sub-micron-scale structures (small N) and micrometer scale structures (larger N). Given that the introduced flexoelectricity is a nonlocal effect, we expect to see size-dependent enhancements at smaller size scales.

We present the flexoelectric size-dependent enhancements, F_{31} and F_{33}, of e_{31} and e_{33}, respectively, for different matrix properties in Figure 3. These are enhancements that are given by:

$$F_{mn} = \frac{e_{mn}(N) - e_{mn}(N=\infty)}{e_{mn}(N=\infty)} \quad (13)$$

where the subscripts m and n correspond to the piezoelectric coefficient in question, $e_{mn}(N = \infty)$ corresponds to the effective piezoelectric coefficient at a large size-scale where flexoelectric effects are absent, and $e_{mn}(N)$ corresponds to the effective piezoelectric coefficient at a particular size-scale. $e_{mn}(N = \infty)$ is obtained here by taking sufficiently large values of N where we notice the absence of size-dependent effects. Eq. 13 represents a relative change in the piezoelectric coefficient as a function of the size-scale parameter N. From Figure 3, we notice that matrices with $\nu_m = 0.35$ show a more pronounced size-dependent enhancement at small size-scales than incompressible matrices with $\nu_m = 0.499$. A plausible explanation for this stems from the fact that the compressible nature of the matrices allows for a better tendency for local deformations that could lead to higher strain gradients and higher flexoelectricity. Furthermore, a common observation across the four subplots is that the size-dependent modifications to the piezoelectric response increase as the matrix material becomes softer indicating. This is because softer matrices have a larger tendency to locally absorb stresses and undergo local deformations building large strain gradients in the process. In the case of the matrices with $\nu_m = 0.35$, we notice that softer matrices with $E_m = 1 \times 10^6$ Pa can lead to nearly a 5-fold improvement in the effective e_{31} piezoelectric coefficient (see Figure 3(a)). In the case of e_{33}, although there is a significant size-dependent effect for $E_m = 1 \times 10^6$ Pa (see Figure 3(c)), the size-dependent effects introduce an effective modification in a direction opposite to the linear piezoelectric effect. A negative value in F_{33} means that the direction of e_{33} has been rotated by 180°.

To obtain a deeper insight into the dependence of the flexoelectric contributions on the matrix properties, we plot the enhancements F_{31} and F_{33} as a function of the Young's modules E_m of the matrix for a size scale $N = 0.2$. This is a small size scale where flexoelectric contributions are noticeable (as seen from Figure 3). One straightforward observation is that the incompressible matrix ($\nu_m =\ 0.499$) shows a very negligible flexoelectric enhancement compared to the compressible matrices. This behavior is relatively more apparent when the enhancements of both the matrices ($\nu_m = 0.35$ and 0.499) are plotted together as shown in Figure 4. A second and more subtle observation is that just as we saw that F_{33} changed signs as we down-scaled the composite geometry, it shows a similar transition in its sign even when Young's modulus is decreased. This implies that depending on how soft or rigid the matrix is, the flexoelectric effect could either act in the same direction of the linear piezoelectricity or the opposite direction.

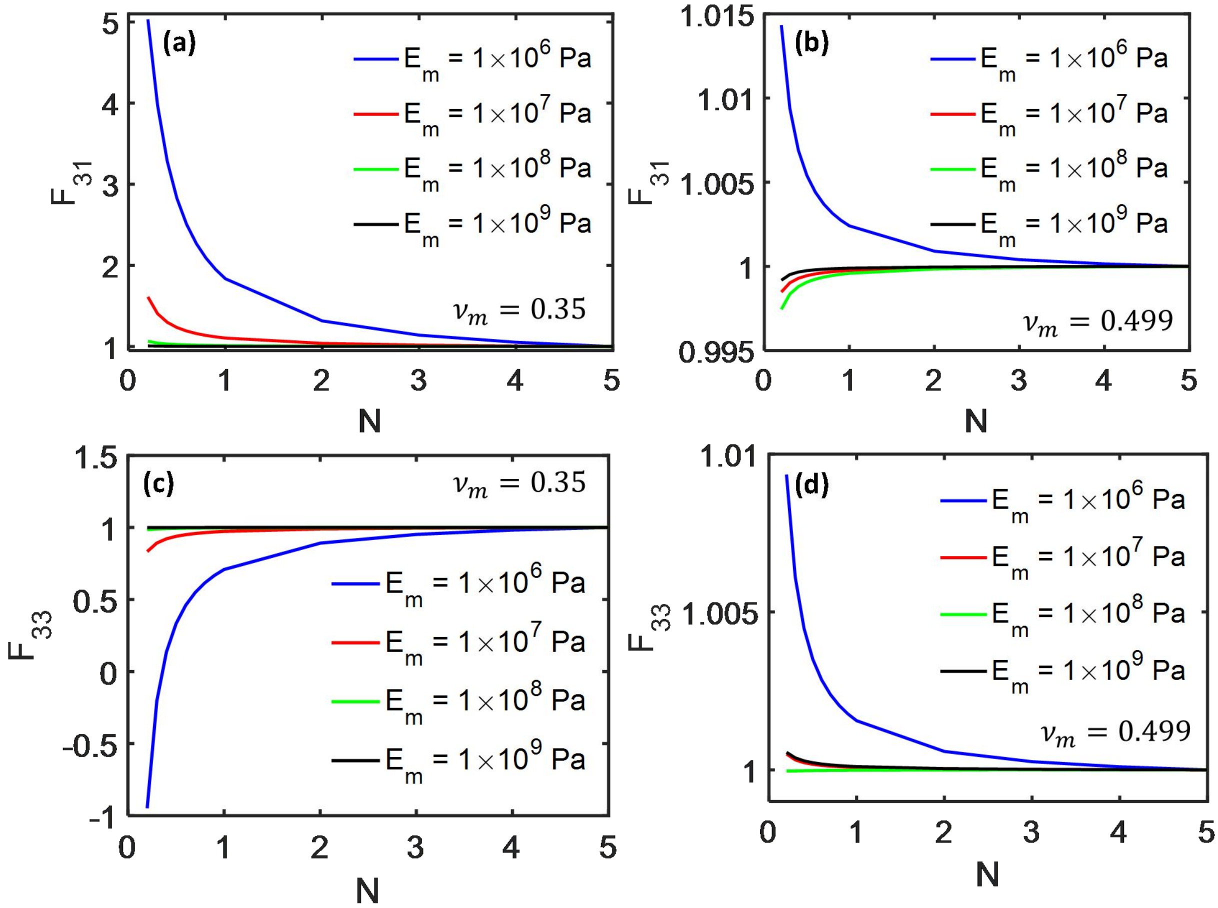

Figure 3 – The flexoelectric enhancements F_{31} and F_{33} in e_{31} and e_{33}, respectively, for different matrix properties E_m and ν_m. (a) and (b) show the enhancements in e_{31} for $\nu_m = 0.35$ and 0.499, respectively, (c) and (d) show the enhancements in e_{33} for $\nu_m = 0.35$ and $\nu_m = 0.499$, respectively.

These observations lead to several important conclusions from the perspective of material design for lead-free piezocomposites:

(a) Firstly, not all matrices that have been reported in the literature in the context of lead-free technologies are conducive to size-dependent piezo-enhancement. Matrix compressibility and matrix softness (lower Young's modulus) are key for higher flexoelectric improvement.

(b) Secondly, the size-dependent piezoelectricity, pronounced at the nonlocal level, and the conventional linear piezoelectricity could counteract depending on the material's anisotropic design.

Based on these conclusions, the design of composites with graded inclusion concentrations can be considered as a promising pathway to enhance the piezoelectric response through size-dependent effects. However, such an effort should always consider the requirements of the application in question to carefully select the composite architecture and the materials comprising the composite.

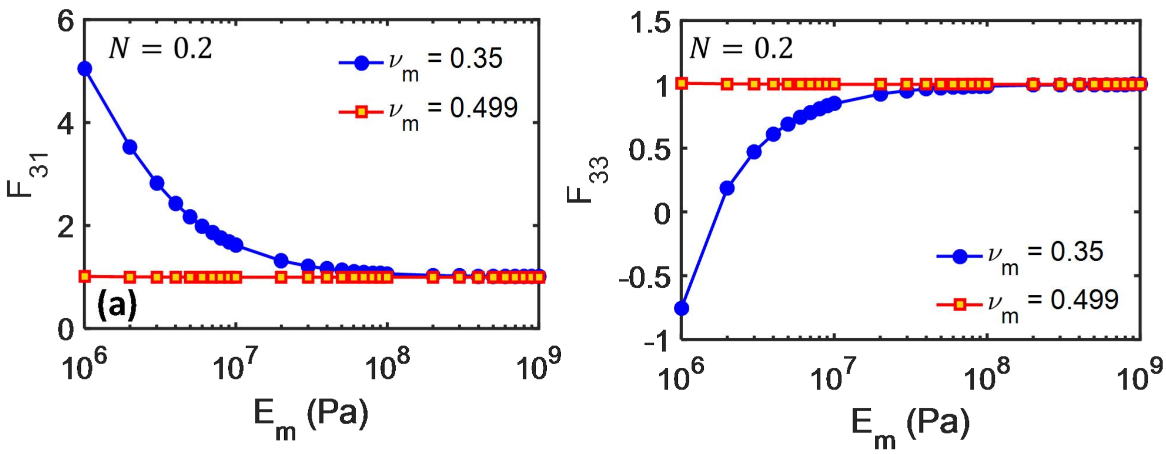

Figure 4 – Flexoelectric enhancements F_{31} (subfigure (a)) and F_{33} (subfigure (b)) for a size-scaled (N=0.2) piezocomposite architecture as a function of Young's modulus E_m of the matrix.

3.2. Size-dependent enhancements in piezocomposites with graded matrix porosities

The idea explored in this section is similar in its principle to the previous idea explored in Section 3.1, with a few major differences. That is, we will introduce a form of mechanical or elastic anisotropy into the composite structure that would lead to strain gradients under the application of forces and, consequently, to flexoelectric coupling. However, the design pathway taken will now be in a different manner. While in section 3.1, we investigated a graded inclusion architecture to bring about the anisotropy, in this section, we will be exploring the introduction of graded porosity in the matrix. As the porosity of the matrix increases, it would have a smaller Young's modulus [55] as desired in a variety of applications such as wearable and soft-robotics [15], leading to a desired elastic gradient. The introduction of porosity in the matrix of a piezocomposite has been explored in the past and has been shown to be effective in improving such characteristics as the hydrostatic piezoelectric figures of merit [56] . However, the effect of porosity in the context of flexoelectricity remains to be investigated systematically. The graded porosity we bring into the design can also be introduced by tuning fabrication parameters in the additive manufacturing techniques [57] and hence the proposed design takes into consideration scalable manufacturing.

To obtain a simple and direct comparison of the flexoelectric effect arising due to porosity, we consider a matrix with a near-homogenous inclusion distribution as a reference composite architecture (see Figure 5(a)). As in the case of the first design proposal discussed in section 3.1, we consider these architectures as representative examples. Owing to the relatively small statistical variations in the piezoelectric response caused by minor variations in the inclusion positions [5], we do not vary the positions of the inclusions and pores for our current analysis. The reference composite architecture presented in Figure 5(a) has an effective inclusion concentration of $V_{BTO} \approx 27\%$. We introduce porosity by simply removing inclusions in a graded fashion as shown in Figure 5(b). The effective inclusion concentration in this architecture is $V_{BTO} \approx 18\%$, which represents a reduced inclusion concentration, where, the volume occupied by the pores is excluded from the calculation of the total volume. For simplicity, as seen in Figure 5(b), pores are introduced in the matrix by removing inclusions from specific positions in the reference composite architecture shown in Figure 5(a).

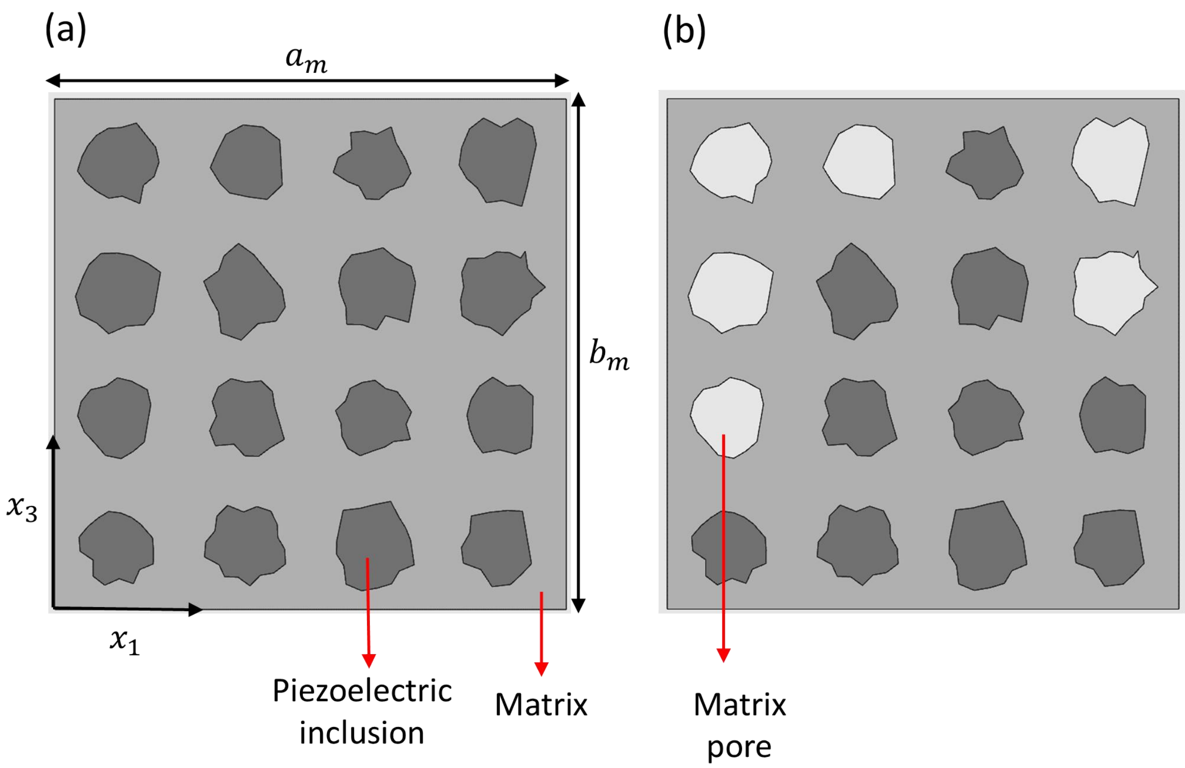

Figure 5 – Piezocomposite architectures considered for investigation in this section: (a) the reference piezocomposite RVE architecture with a near-homogenous inclusion concentration, and (b) A piezocomposite with a graded porosity that increases along the x_3 direction.

We compute the effective piezoelectric coefficients e_{31} and e_{33} as highlighted in section 2. We further compute the size-dependent enhancements in these quantities. We carry out these calculations for a soft hydrogel-like matrix with $E_m = 1 \times 10^6$ Pa, for the purposes of illustration. The results are shown in Figure 6(a)-(d) for two cases of Poisson's ratio: $\nu_m = 0.35$ and $\nu_m = 0.499$.

Firstly, we notice that the non-porous matrix also has some size-dependent enhancements. This is due to the random shapes and placements of the inclusions which results in a small net anisotropy. However, the introduction of porosity in the matrix shows that there is a more pronounced enhancement in the flexoelectric contribution. Besides, we also notice that the flexoelectric enhancement may noticeably improve the piezoelectric response as demonstrated by Figure 6(a) and (d). In fact, we see a more than 10-fold increase in the effective e_{31} of the matrix with $\nu_m = 0.35$ and a more than 25% increase in the effective e_{33} of the matrix with $\nu_m = 0.499$. Notably, the introduction of pores in the matrix enables a much larger flexoelectric enhancement in the case of the incompressible matrix compared to the previous design which only resulted in a very marginal flexoelectric contribution. In the remaining two cases (Figure 6(b) and (c)), the flexoelectric component opposes the linear piezoelectric response and can cause an eventual change in the sign of the effective piezoelectric coefficients. Therefore, as in the case of the design with graded inclusion concentrations, discussed in section 3.1, one needs to carefully define the requirements of the piezocomposite material in advance to tune the compositional and structural details of the porosity of the matrix.

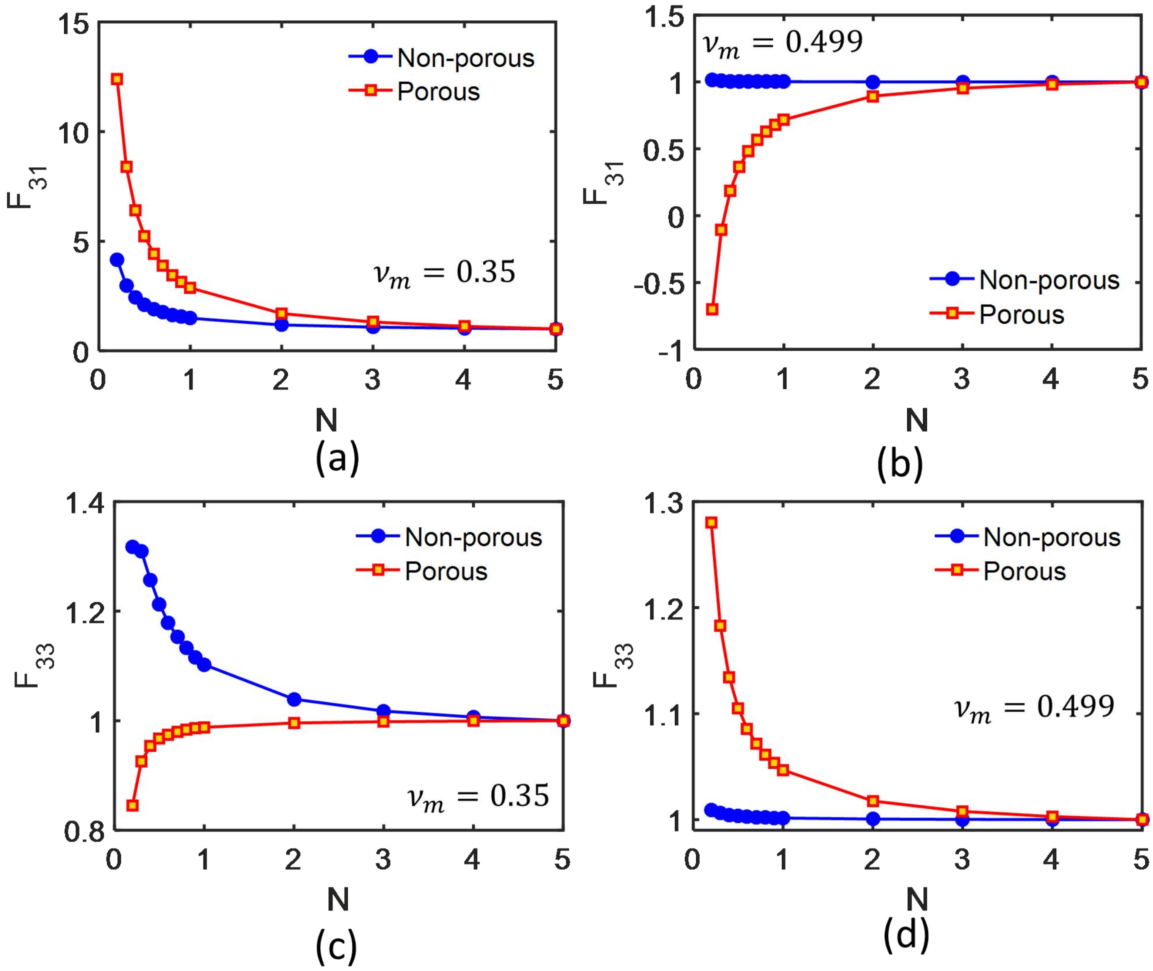

Figure 6 – Size-dependent enhancement to the effective piezoelectricity: (a)-(b): Enhancements in e_{31} for matrices with $\nu_m = 0.35$ and $\nu_m = 0.499$, respectively, (c)-(d): Enhancements in e_{33} for matrices with $\nu_m = 0.35$ and $\nu_m = 0.499$, respectively

In summary, the introduction of porosity in the matrix can lead to considerable flexoelectric improvements in both regular compressible matrices and incompressible matrices and this could be a relatively more material-agnostic design principle compared to the design proposed in section 3.1.

4. Conclusions

We have systematically explored two compelling design principles to introduce flexoelectric enhancement in lead-free piezoelectric composites. The guiding requirements were, firstly, to explore pathways for improvements in the piezoelectric response by avoiding the use of excessive inclusion concentrations and matrix-hardening nanomaterials, and secondly, to conceptualize material structures and compositions that can be easily manufactured by simply tuning the parameters of emerging techniques such as additive manufacturing. The first of the proposals involves a graded inclusion concentration, and the second proposal involves the introduction of graded matrix porosity in the composite architecture. We observe, through our investigations, that while both proposals lead to flexoelectric contributions, the nature of the structural and compositional inhomogeneity introduced can lead to a size-dependent flexoelectric component that either opposes or reinforces the existing linear piezoelectric response of the composite. In the cases where there is flexoelectric reinforcement, we notice that it is more significant in compressible matrices than in incompressible matrices. Secondly, we also notice that the introduction of graded porosity leads to a much more pronounced flexoelectric reinforcement in composites with incompressible matrices than the design with a graded inclusion concentration. Our presented proposals and experiments suggest that there are potentially many ways in which an elastic/mechanical anisotropy can be introduced in a piezocomposite architecture that leads to flexoelectric enhancements. Further, the designs considered here target improving the piezoelectric response while not compromising on the softness of the matrices, which is particularly important in the context of compliant structural integration and wearable applications of piezoelectric sensors, actuators, and energy harvesters. We strongly believe that the material-agnostic design pathways proposed here represent a paradigm shift in designing efficient lead-free ecologically friendly technologies by tapping into coupled phenomena that are specifically active at smaller length scales that can be introduced through optimal structuring of materials. The findings have laid ground for the study of more complex hierarchical material patterns involving thermally stabler alternative lead-free piezoelectric materials which have considerable potential to bring about flexoelectric enhancements in eco-friendly composite materials.

Acknowledgements

This work was supported by the Consejería de Transformación Económica, Industria, Conocimiento y Universidades de la Junta de Andalucía (Spain) through the research project P18-RT-3128. The project was co-funded by the European Regional Development Fund (ERDF). RM and AKJ are also grateful to the NSERC and CRC program for their support

References

[1] D. Maurya *et al.*, “Lead-free piezoelectric materials and composites for high power density energy harvesting,” *J Mater Res*, vol. 33, no. 16, pp. 2235–2263, Aug. 2018, doi: 10.1557/jmr.2018.172.

[2] T. Ibn-Mohammed *et al.*, “Are lead-free piezoelectrics more environmentally friendly?,” *MRS Commun*, vol. 7, no. 1, pp. 1–7, Mar. 2017, doi: 10.1557/mrc.2017.10.

[3] D. Maurya, Y. Zhou, Y. Yan, and S. Priya, "Synthesis mechanism of grain-oriented lead-free piezoelectric Na0.5Bi0.5TiO3–BaTiO3 ceramics with giant piezoelectric response," *J Mater Chem C Mater*, vol. 1, no. 11, p. 2102, 2013, doi: 10.1039/c3tc00619k.

[4] P. Zheng, J. L. Zhang, Y. Q. Tan, and C. L. Wang, "Grain-size effects on dielectric and piezoelectric properties of poled BaTiO3 ceramics," *Acta Mater*, vol. 60, no. 13–14, pp. 5022–5030, Aug. 2012, doi: 10.1016/j.actamat.2012.06.015.

[5] J. A. Krishnaswamy, F. C. Buroni, F. Garcia-Sanchez, R. Melnik, L. Rodriguez-Tembleque, and A. Saez, "Improving the performance of lead-free piezoelectric composites by using polycrystalline inclusions and tuning the dielectric matrix environment," *Smart Mater Struct*, vol. 28, no. 7, p. 075032, Jul. 2019, doi: 10.1088/1361-665X/ab1f14.

[6] J. A. Krishnaswamy, F. C. Buroni, F. Garcia-Sanchez, R. Melnik, L. Rodriguez-Tembleque, and A. Saez, "Lead-free piezocomposites with CNT-modified matrices: Accounting for agglomerations and molecular defects," *Compos Struct*, vol. 224, p. 111033, Sep. 2019, doi: 10.1016/j.compstruct.2019.111033.

[7] H. Kim *et al.*, "Increased piezoelectric response in functional nanocomposites through multiwall carbon nanotube interface and fused-deposition modeling three-dimensional printing," *MRS Commun*, vol. 7, no. 4, pp. 960–966, Dec. 2017, doi: 10.1557/mrc.2017.126.

[8] Q. Li, Y. Kuang, and M. Zhu, "Auxetic piezoelectric energy harvesters for increased electric power output," *AIP Adv*, vol. 7, no. 1, p. 015104, Jan. 2017, doi: 10.1063/1.4974310.

[9] E. P. HADJIGEORGIOU and G. E. STAVROULAKIS, "THE USE OF AUXETIC MATERIALS IN SMART STRUCTURES," *Computational Methods in Science and Technology*, vol. 10, no. 2, pp. 147–160, 2004, doi: 10.12921/cmst.2004.10.02.147-160.

[10] S. Mao and P. K. Purohit, "Insights Into Flexoelectric Solids From Strain-Gradient Elasticity," *J Appl Mech*, vol. 81, no. 8, Aug. 2014, doi: 10.1115/1.4027451.

[11] N. D. Sharma, C. M. Landis, and P. Sharma, "Piezoelectric thin-film superlattices without using piezoelectric materials," *J Appl Phys*, vol. 108, no. 2, p. 024304, Jul. 2010, doi: 10.1063/1.3443404.

[12] X. Liang, S. Hu, and S. Shen, "Effects of surface and flexoelectricity on a piezoelectric nanobeam," *Smart Mater Struct*, vol. 23, no. 3, p. 035020, Mar. 2014, doi: 10.1088/0964-1726/23/3/035020.

[13] A. Abdollahi, N. Domingo, I. Arias, and G. Catalan, "Converse flexoelectricity yields large piezoresponse force microscopy signals in non-piezoelectric materials," *Nat Commun*, vol. 10, no. 1, p. 1266, Dec. 2019, doi: 10.1038/s41467-019-09266-y.

[14] J. A. Krishnaswamy, L. Rodriguez-Tembleque, R. Melnik, F. C. Buroni, and A. Saez, "Size dependent electro-elastic enhancement in geometrically anisotropic lead-free piezocomposites," *Int J Mech Sci*, vol. 182, p. 105745, Sep. 2020, doi: 10.1016/j.ijmecsci.2020.105745.

[15] M. Grasinger, K. Mozaffari, and P. Sharma, "Flexoelectricity in soft elastomers and the molecular mechanisms underpinning the design and emergence of giant flexoelectricity,"

Proceedings of the National Academy of Sciences, vol. 118, no. 21, May 2021, doi: 10.1073/pnas.2102477118.

[16] H. Wu, Y. Zhang, J. Wu, J. Wang, and S. J. Pennycook, "Microstructural Origins of High Piezoelectric Performance: A Pathway to Practical Lead-Free Materials," *Adv Funct Mater*, vol. 29, no. 33, p. 1902911, Aug. 2019, doi: 10.1002/adfm.201902911.

[17] X. Lv, X. Zhang, and J. Wu, "Nano-domains in lead-free piezoceramics: a review," *J Mater Chem A Mater*, vol. 8, no. 20, pp. 10026–10073, 2020, doi: 10.1039/D0TA03201H.

[18] Z. Kuang, "Internal energy variational principles and governing equations in electroelastic analysis," *Int J Solids Struct*, vol. 46, no. 3–4, pp. 902–911, Feb. 2009, doi: 10.1016/j.ijsolstr.2008.10.001.

[19] B. He, B. Javvaji, and X. Zhuang, "Characterizing Flexoelectricity in Composite Material Using the Element-Free Galerkin Method," *Energies (Basel)*, vol. 12, no. 2, p. 271, Jan. 2019, doi: 10.3390/en12020271.

[20] A. Abdollahi, C. Peco, D. Millán, M. Arroyo, and I. Arias, "Computational evaluation of the flexoelectric effect in dielectric solids," *J Appl Phys*, vol. 116, no. 9, p. 093502, Sep. 2014, doi: 10.1063/1.4893974.

[21] M. Bahrami-Samani, S. R. Patil, and R. Melnik, "Higher-order nonlinear electromechanical effects in wurtzite GaN/AlN quantum dots," *Journal of Physics: Condensed Matter*, vol. 22, no. 49, p. 495301, Dec. 2010, doi: 10.1088/0953-8984/22/49/495301.

[22] S. Prabhakar, RoderickV. N. Melnik, P. Neittaanmäki, and T. Tiihonen, "Coupled Magneto-Thermo-Electromechanical Effects and Electronic Properties of Quantum Dots," *J Comput Theor Nanosci*, vol. 10, no. 3, pp. 534–547, Mar. 2013, doi: 10.1166/jctn.2013.2731.

[23] J. Sladek, V. Sladek, and S. M. Hosseini, "Analysis of a curved Timoshenko nano-beam with flexoelectricity," *Acta Mech*, vol. 232, no. 4, pp. 1563–1581, Apr. 2021, doi: 10.1007/s00707-020-02901-6.

[24] X. Tian, J. Sladek, V. Sladek, Q. Deng, and Q. Li, "A collocation mixed finite element method for the analysis of flexoelectric solids," *Int J Solids Struct*, vol. 217–218, pp. 27–39, May 2021, doi: 10.1016/j.ijsolstr.2021.01.031.

[25] T. Profant, J. Sládek, V. Sládek, and M. Kotoul, "Assessment of amplitude factors of asymptotic expansion at crack tip in flexoelectric solid under mode I and II loadings," *Int J Solids Struct*, vol. 269, p. 112194, May 2023, doi: 10.1016/j.ijsolstr.2023.112194.

[26] X. Tian *et al.*, "Analytical Studies on Mode III Fracture in Flexoelectric Solids," *J Appl Mech*, vol. 89, no. 4, Apr. 2022, doi: 10.1115/1.4053268.

[27] R. Maranganti and P. Sharma, "Length Scales at which Classical Elasticity Breaks Down for Various Materials," *Phys Rev Lett*, vol. 98, no. 19, p. 195504, May 2007, doi: 10.1103/PhysRevLett.98.195504.

[28] N. D. Sharma, R. Maranganti, and P. Sharma, “On the possibility of piezoelectric nanocomposites without using piezoelectric materials,” *J Mech Phys Solids*, vol. 55, no. 11, pp. 2328–2350, Nov. 2007, doi: 10.1016/j.jmps.2007.03.016.

[29] J. A. Krishnaswamy, L. Rodriguez-Tembleque, R. Melnik, F. C. Buroni, and A. Saez, “Size dependent electro-elastic enhancement in geometrically anisotropic lead-free piezocomposites,” *Int J Mech Sci*, vol. 182, p. 105745, Sep. 2020, doi: 10.1016/j.ijmecsci.2020.105745.

[30] K. Tannhäuser, P. H. Serrao, and S. Kozinov, “Second-Order Collocation-Based Mixed FEM for Flexoelectric Solids,” *Solids*, vol. 4, no. 1, pp. 39–70, Feb. 2023, doi: 10.3390/solids4010004.

[31] J. López, N. Valizadeh, and T. Rabczuk, “An isogeometric phase–field based shape and topology optimization for flexoelectric structures,” *Comput Methods Appl Mech Eng*, vol. 391, p. 114564, Mar. 2022, doi: 10.1016/j.cma.2021.114564.

[32] M. Kim, “A Numerical Framework for Geometrically Nonlinear Deformation of Flexoelectric Solids Immersed in an Electrostatic Medium,” *J Appl Mech*, vol. 88, no. 8, Aug. 2021, doi: 10.1115/1.4050688.

[33] D. Codony, O. Marco, S. Fernández-Méndez, and I. Arias, “An immersed boundary hierarchical B-spline method for flexoelectricity,” *Comput Methods Appl Mech Eng*, vol. 354, pp. 750–782, Sep. 2019, doi: 10.1016/j.cma.2019.05.036.

[34] J. Yvonnet and L. P. Liu, “A numerical framework for modeling flexoelectricity and Maxwell stress in soft dielectrics at finite strains,” *Comput Methods Appl Mech Eng*, vol. 313, pp. 450–482, Jan. 2017, doi: 10.1016/j.cma.2016.09.007.

[35] A. A. Saputra, V. Sladek, J. Sladek, and C. Song, “Micromechanics determination of effective material coefficients of cement-based piezoelectric ceramic composites,” *J Intell Mater Syst Struct*, vol. 29, no. 5, pp. 845–862, Mar. 2018, doi: 10.1177/1045389X17721047.

[36] C.-H. Hong *et al.*, “Lead-free piezoceramics – Where to move on?,” *Journal of Materiomics*, vol. 2, no. 1, pp. 1–24, Mar. 2016, doi: 10.1016/j.jmat.2015.12.002.

[37] Binghao Guo, “Flexoelectricity in Polycrystalline SrTiO3 Ceramics,” Northwestern University, 2019.

[38] J. Narvaez, F. Vasquez-Sancho, and G. Catalan, “Enhanced flexoelectric-like response in oxide semiconductors,” *Nature*, vol. 538, no. 7624, pp. 219–221, Oct. 2016, doi: 10.1038/nature19761.

[39] N. A. Filatov, D. v Nozdriukhin, and A. S. Bukatin, “The kinetic study of solidification PEGDA microparticles in flow-focusing microfluidic chip,” *J Phys Conf Ser*, vol. 917, p. 042024, Nov. 2017, doi: 10.1088/1742-6596/917/4/042024.

[40] D. Quan, J. L. Urdániz, and A. Ivanković, “Enhancing mode-I and mode-II fracture toughness of epoxy and carbon fibre reinforced epoxy composites using multi-walled carbon nanotubes,” *Mater Des*, vol. 143, pp. 81–92, Apr. 2018, doi: 10.1016/j.matdes.2018.01.051.

[41] R. H. Pritchard, P. Lava, D. Debruyne, and E. M. Terentjev, "Precise determination of the Poisson ratio in soft materials with 2D digital image correlation," *Soft Matter*, vol. 9, no. 26, p. 6037, 2013, doi: 10.1039/c3sm50901j.

[42] S. Kim *et al.*, "Revisit to three-dimensional percolation theory: Accurate analysis for highly stretchable conductive composite materials," *Sci Rep*, vol. 6, no. 1, p. 34632, Dec. 2016, doi: 10.1038/srep34632.

[43] A. Abdollahi, C. Peco, D. Millán, M. Arroyo, and I. Arias, "Computational evaluation of the flexoelectric effect in dielectric solids," *J Appl Phys*, vol. 116, no. 9, p. 093502, Sep. 2014, doi: 10.1063/1.4893974.

[44] L. Shu, X. Wei, T. Pang, X. Yao, and C. Wang, "Symmetry of flexoelectric coefficients in crystalline medium," *J Appl Phys*, vol. 110, no. 10, p. 104106, Nov. 2011, doi: 10.1063/1.3662196.

[45] T. D. Nguyen, S. Mao, Y.-W. Yeh, P. K. Purohit, and M. C. McAlpine, "Nanoscale Flexoelectricity," *Advanced Materials*, vol. 25, no. 7, pp. 946–974, Feb. 2013, doi: 10.1002/adma.201203852.

[46] R. Maranganti and P. Sharma, "Atomistic determination of flexoelectric properties of crystalline dielectrics," *Phys Rev B*, vol. 80, no. 5, p. 054109, Aug. 2009, doi: 10.1103/PhysRevB.80.054109.

[47] H. v. Do, T. Lahmer, X. Zhuang, N. Alajlan, H. Nguyen-Xuan, and T. Rabczuk, "An isogeometric analysis to identify the full flexoelectric complex material properties based on electrical impedance curve," *Comput Struct*, vol. 214, pp. 1–14, Apr. 2019, doi: 10.1016/j.compstruc.2018.10.019.

[48] A. Luna *et al.*, "Giant Electrostrictive Response and Piezoresistivity of Emulsion Templated Nanocomposites," *Langmuir*, vol. 33, no. 18, pp. 4528–4536, May 2017, doi: 10.1021/acs.langmuir.6b04185.

[49] Wrutu Deepak Parulkar, "Electromechanical Characterization of Poly(Dimethyl Siloxane) Based Electroactive Polymers," Virginia Commonwealth University, 2005.

[50] S. P. Joshi, "Non-linear constitutive relations for piezoceramic materials," *Smart Mater Struct*, vol. 1, no. 1, pp. 80–83, Mar. 1992, doi: 10.1088/0964-1726/1/1/012.

[51] J. Y. Li, "The effective electroelastic moduli of textured piezoelectric polycrystalline aggregates," *J Mech Phys Solids*, vol. 48, no. 3, pp. 529–552, Mar. 2000, doi: 10.1016/S0022-5096(99)00042-3.

[52] T. Hu, Q. Deng, X. Liang, and S. Shen, "Measuring the flexoelectric coefficient of bulk barium titanate from a shock wave experiment," *J Appl Phys*, vol. 122, no. 5, p. 055106, Aug. 2017, doi: 10.1063/1.4997475.

[53] B. Chu and D. R. Salem, "Flexoelectricity in several thermoplastic and thermosetting polymers," *Appl Phys Lett*, vol. 101, no. 10, p. 103905, Sep. 2012, doi: 10.1063/1.4750064.

[54] H. Cui *et al.*, "Three-dimensional printing of piezoelectric materials with designed anisotropy and directional response," *Nat Mater*, vol. 18, no. 3, pp. 234–241, Mar. 2019, doi: 10.1038/s41563-018-0268-1.

[55] L. S. Morrissey and S. Nakhla, "A Finite Element Model to Predict the Effect of Porosity on Elastic Modulus in Low-Porosity Materials," *Metallurgical and Materials Transactions A*, vol. 49, no. 7, pp. 2622–2630, Jul. 2018, doi: 10.1007/s11661-018-4623-2.

[56] Y.-C. Chen, K.-K. Chang, L. Wu, and C.-L. Huang, "Effects of porosity and polymer matrix on the properties of piezoelectric ceramic/polymer composites," *Ferroelectrics*, vol. 215, no. 1, pp. 123–130, Jul. 1998, doi: 10.1080/00150199808229556.

[57] R. Baptista and M. Guedes, "Morphological and mechanical characterization of 3D printed PLA scaffolds with controlled porosity for trabecular bone tissue replacement," *Materials Science and Engineering: C*, vol. 118, p. 111528, Jan. 2021, doi: 10.1016/j.msec.2020.111528.